Tuning the activity of known drugs via the introduction of halogen atoms, a case study of SERT ligands − Fluoxetine and fluvoxamine

Jakub Staroń[*], Wojciech Pietruś, Ryszard Bugno, Rafał Kurczab, Grzegorz Satała, Dawid Warszycki, Tomasz Lenda, Anna Wantuch, Adam S. Hogendorf, Agata Hogendorf, Beata Duszyńska, Andrzej J. Bojarski

Maj Institute of Pharmacology, Polish Academy of Sciences, 12 Smętna Street, 31-343, Kraków, Poland

ABSTRACT

The selective serotonin reuptake inhibitors (SSRIs), acting at the serotonin transporter (SERT), are one of the most widely prescribed antidepressant medications. All five approved SSRIs possess either fluorine or chlorine atoms, and there is a limited number of reports describing their analogs with heavier halogens, i.e., bromine and iodine. To elucidate the role of halogen atoms in the binding of SSRIs to SERT, we designed a series of 22 fluoxetine and fluvoxamine analogs substituted with fluorine, chlorine, bromine, and iodine atoms, differently arranged on the phenyl ring. The obtained biological activity data, supported by a thorough *in silico* binding mode analysis, allowed the identification of two partners for halogen bond interactions: the backbone carbonyl oxygen atoms of E493 and T497. Additionally, compounds with heavier halogen atoms were found to bind with the SERT via a distinctly different binding mode, a result not presented elsewhere. The subsequent analysis of the prepared XSAR sets showed that E493 and T497 participated in the largest number of formed halogen bonds. The XSAR library analysis led to the synthesis of two of the most active compounds (3,4-diCl-fluoxetine **42**, SERT K_i = 5 nM and 3,4-diCl-fluvoxamine **46**, SERT K_i = 9 nM, fluoxetine SERT K_i = 31 nM, fluvoxamine SERT K_i = 458 nM). We present an example of the successful use of a rational methodology to analyze binding and design more active compounds by halogen atom introduction. 'XSAR library analysis', a new tool in medicinal chemistry, was instrumental in identifying optimal halogen atom substitution.

© 2021 Elsevier Masson SAS. All rights reserved.

1. Introduction

Serotonin transporter (SERT) is a monoamine transporter-type protein composed of a 630 amino acid chain that forms 12 transmembrane domains [1,2]. It is located at the presynaptic axon terminal and somatodendritic end of neurons [3] and regulates serotonin transmission by removing serotonin from the extracellular space [2]. Extensive research has shown that patients with a functional polymorphism in the promoter region of the SERT gene exhibit more depressive behavior in response to life events, thus supporting the role of SERT in the regulation of mood disorders [4,5].

Halogen atoms are among the most popular substituents utilized for the optimization of the properties of biologically active compounds. They can form both hydrophobic and electrostatic interactions with biological targets. The latter are mainly represented by the halogen bond, which according to IUPAC definition is "a net attractive interaction between an electrophilic region associated with a halogen atom in a molecular entity and a nucleophilic region in another, or the same, molecular entity" [6]. In particular, the halogen bond is formed between the electron deficiency region, called the σ-hole, on top of the halogen atom and a Lewis base, most often oxygen from the carbonyl group of the peptide chain [7,8]. The size of the σ-hole strictly determines the strength of the halogen bond. It is greatest for iodine and smallest for chlorine. Moreover, its size can be modified by the introduction of neighboring electron-withdrawing groups. Several studies have shown that additional fluorine atoms in halobenzenes greatly increase the size of the σ-hole [9–11]. The construction of a halogen bond strictly defines its geometry. The optimal interaction is of near linear nature, where the angle donor (D)-halogen (X)···acceptor (A) is 160−180° and the distance between halogen and acceptor is

much shorter than the sum of atomic van der Waals radii (80%) and is equal to 3.06 Å for chlorine, 3.15 Å for bromine and 3.24 Å for iodine [12].

All five approved selective serotonin reuptake inhibitors (SSRIs) possess halogen atom(s) in their structure (Fig. 1); four possess fluorine and one a chlorine atom. A limited number of biological activity data of SSRI analogs with heavier halogens can be found, and no consistent conclusion on the significance of halogen(s) can be derived. Substitution of fluorine for chlorine in citalopram caused a slight increase in binding affinity ($IC_{50} = 59$ nM [13] to $IC_{50} = 49$ nM [13], respectively), whereas introduction of a bromine decreased it ($IC_{50} = 121$ nM [13]). In the case of fluoxetine (SERT $K_i = 17$ nM [14]), replacement of the trifluoromethyl group with fluorine and chlorine caused a decrease in binding affinity ($K_i = 142$ nM [14] and 638 nM [14], respectively), while an iodine

derivative exhibited a slight increase in binding affinity ($K_i = 14.4$ nM [15]). Fluvoxamine substitutions with fluorine, chlorine, and bromine can be found in the patent literature, but no complimentary biological data allowing comparison are available [16]. In turn, the SAR of the different halogenated modafinil analogs can be found in a study by Okunola-Bakare et al., where substitution of chlorine with bromine slightly increased the binding affinity to SERT (29.8 nM for chlorine derivative and 26.1 nM for bromine derivative) [17]. Additionally, biological data for bromo-paroxetine were also reported. Substitution of fluorine to bromine decreased the binding affinity 13-fold (from $K_i = 0.08$ nM, for paroxetine to $K_i = 1.07$ nM for Br-paroxetine); however, the new compound maintained high activity [18]. A survey of the ChEMBL database (release 25) revealed that out of 3529 stored SERT ligands (with activity < 1000 nM), 145 contain the CF_3 group, 768 contain fluorine, 1207 contain chlorine, 101 contain bromine, and 48 contain iodine. It is apparent that there are significantly fewer derivatives with heavier halogens − bromine and iodine − than with fluorine, despite their often greater affinity for SERT. The small number of heavier halogens can be explained by a general tendency in the pharmaceutical industry to avoid these atoms in drug chemical structures.

Even less information can be found regarding the analysis of the role of halogen atoms in binding to SERT. The only remark about a halogen binding pocket in SERT was published in 2009 by Zhou et al. in a study investigating the specificity of serotonin transporter inhibitors: sertraline and both isomers of fluoxetine [19]. Zhou et al. found that SSRIs bind to the extracellular vestibule in the LeuT protein (a bacterial leucine transporter) in a manner in which halogen atoms from all compounds align in a pocket formed by L25, G26, L29, R30, Y108, I111, and F253, which was called the halogen binding pocket (HBP). Moreover, the HBP sequence homology
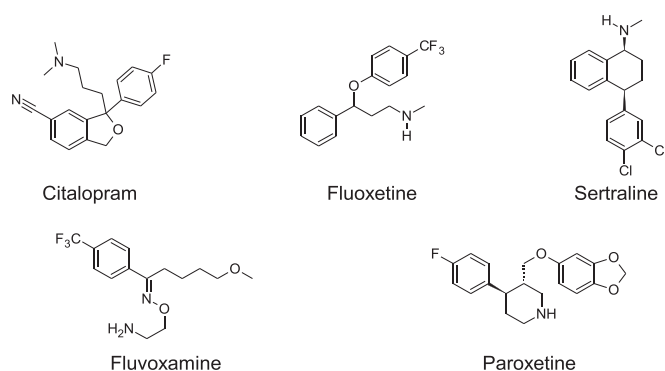
Fig. 1. Structures of FDA-approved selective serotonin reuptake inhibitors (data from http://www.fda.gov/Drugs/DrugSafety/InformationbyDrugClass/ucm283587.htm).
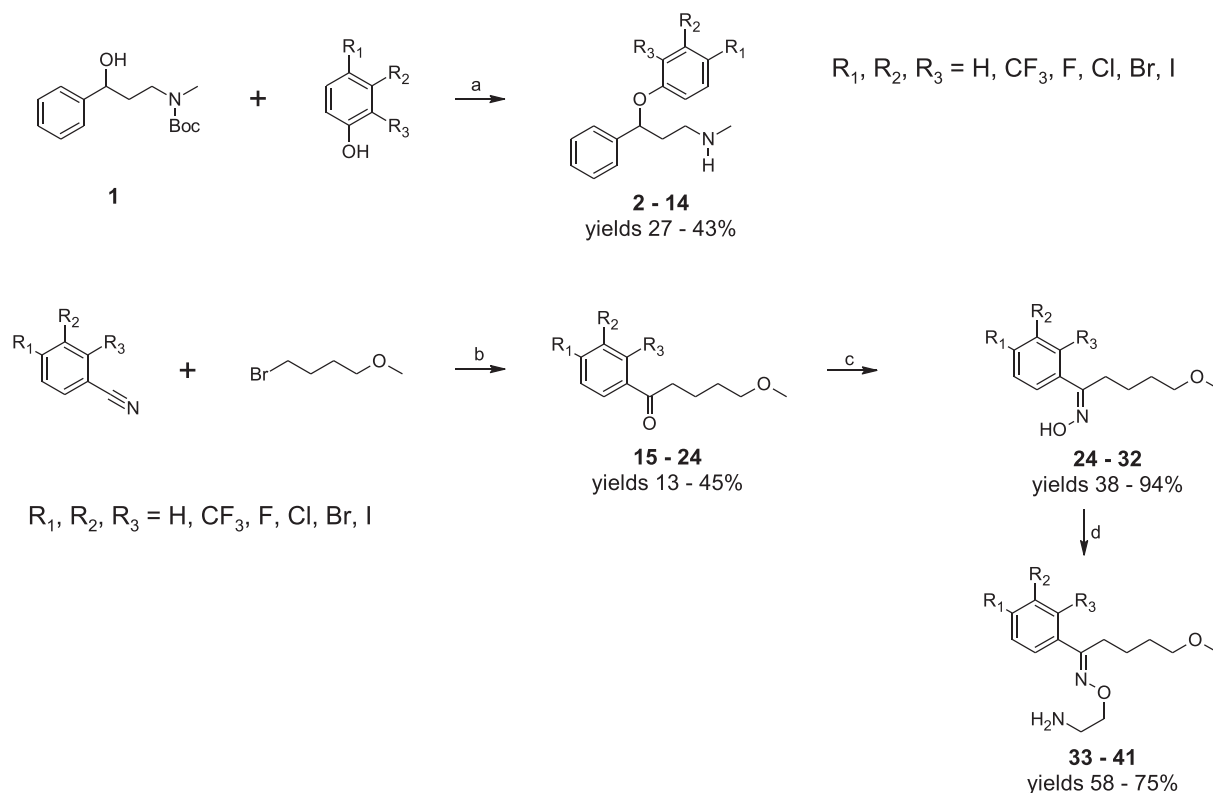
Scheme 1. Synthesis of fluoxetine and fluvoxamine analogs. (a) PPh₃, DIAD, THF, conc. H₃PO₄, rt; (b) Mg, Et₂O, reflux; (c) NH₂OH·HCl, NaOAc, EtOH, rt; (d) 2-chloroethylamine hydrochloride, KOH, DMF, rt.

between LeuT, SERT, NET, and DAT is high. The only difference between NET (norepinephrine transporter), DAT (dopamine transporter), and SERT is one amino acid, i.e., A77, A81, and G100, respectively. This suggested that in human SERT, these SSRIs might bind similarly. To test their hypothesis, Zhou et al. analyzed the binding of SSRIs to SERT mutants with, among others, mutated amino acids forming or neighboring the HBP. All reported mutations caused a decrease in affinity.

In this study, we performed an analysis of halogen substitution on two of the FDA-approved (Food and Drug Administration) SSRIs, fluoxetine and fluvoxamine, to investigate the role of halogen atoms in SERT ligand binding. In the synthesized fluoxetine and fluvoxamine analogs, the trifluoromethyl group was substituted with fluorine, chlorine, bromine, and iodine. Moreover, for chlorine, bromine, and iodine derivatives, an additional fluorine atom was introduced to alter the electron density distribution on the halogen atom. Here, the results of a radioligand displacement binding experiment performed for SERT and an analysis of the binding mode based on induced fit docking and molecular dynamics are presented.

2. Chemistry

Fluoxetine, together with its analogs, was synthesized using a two-step, one-pot procedure involving a Mitsunobu reaction of *tert*-butyl *N*-(3-hydroxy-3-phenylpropyl)-*N*-methylcarbamate with appropriate phenol and subsequent deprotection (Scheme 1). In turn, the synthesis of fluvoxamine analogs consisted of three steps: Grignard reaction of 1-bromo-4-methoxybutane with appropriate nitrile, condensation with hydroxylamine, and finally, substitution with 2-chloroethylamine (Scheme 1).

3. Results

3.1. Biological activity

Binding affinity constants for SERT were measured using a radioligand displacement experiment (Table 1). Among the synthesized analogs, the exchange of trifluoromethyl groups into heavier halogens (chlorine, bromine, and iodine) generally causes an increase in binding affinity (Fig. 2). Additionally, the simultaneous introduction of a fluorine atom results in more active compounds (**13**, **14**, **38**–**41**). This is true for all compounds except the 2,4-substitution of fluoxetine, where the fluorine atom decreases the binding affinity 1.6- and 1.3-fold (compounds **10** and **11**, respectively). Changing the CF$_3$ group into a fluorine atom in both cases (compounds **4** and **34**) lowers the binding affinity 17- and 3.5-fold, respectively. In turn, shifting the fluorine to the C-3 position in fluoxetine analog **5** slightly increases (1.9-fold) the binding affinity. A similar effect can be observed in the case of 3-chloro fluoxetine analog **7**, with a 1.2-fold increase.

3.2. Molecular modeling

An induced fit docking protocol (IFD) was used to investigate the phenomenon behind the observed structure-activity relationship. The protocol utilized the SERT model based on the SERT crystal structure (PDB ID: 5I6X). Among all of the ligand poses that were returned, each of the docked analogs was found in two different binding modes (Fig. 3). In the first mode, the compound is located analogously, as can be found in the published crystal structures of SERT-SSRI complexes [20,21]. The trifluoromethyl/halogen moiety is located in a lipophilic pocket between helixes TM3 and TM8, surrounded by residues I172, A173, Y176, and L443, and the basic nitrogen atom forms a hydrogen bond with aspartic acid D98. In the

Table 1
Binding affinity values for synthesized fluoxetine and fluvoxamine analogs.
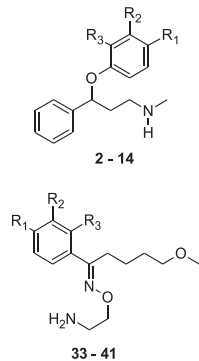
Cmpd	R$_1$	R$_2$	R$_3$	SERT K_i [nM]
2 (ST-213)	H	H	H	1458
3^a (ST-129)	CF$_3$	H	H	31
4 (ST-143)	F	H	H	543
5 (ST-215)	H	F	H	349
6 (ST-141)	Cl	H	H	55
7 (ST-214)	H	Cl	H	66
8 (ST-132)	Br	H	H	24
9 (ST-137)	I	H	H	14
10 (ST-130)	Cl	H	F	52
11 (ST-133)	Br	H	F	41
12 (ST-138)	I	H	F	23
13 (ST-131)	Cl	F	H	31
14 (ST-134)	Br	F	H	19
33^b (ST-110)	CF$_3$	H	H	458
34 (ST-111)	F	H	H	1617
35 (ST-112)	Cl	H	H	61
36 (ST-113)	Br	H	H	23
37 (ST-201)	I	H	H	15
38 (ST-118)	Cl	H	F	202
39 (ST-121)	Br	H	F	137
40 (ST-119)	Cl	F	H	62
41 (ST-120)	Br	F	H	21

Binding affinity, K_i, expressed as the average of at least two independent experiments; the maximum S.D. did not exceed 10% (see Supplementary Information, page 20, Table 4).
^{a} Fluoxetine.
^{b} Fluvoxamine.

case of the fluoxetine complex, the phenyl ring lies in proximity to F335 and F341. In turn, the oxygen atom of the fluvoxamines' methoxybutyl chain forms a hydrogen bond with the hydroxyl group of Y175. In the second mode, the compound is flipped, and now the trifluoromethyl/halogen moiety is directed towards helix TM10, pointing into residues E493 or T497. In this position, the halogen atom (chlorine, bromine) was found to be engaged in a halogen bond with the backbone oxygen of these residues. In turn, the iodine atom of **9** positioned itself between helixes TM10 and TM3, where it is surrounded by a net of interactions with three residues: hydroxyl of T497, guanidine of R104, and hydroxyl of T176. In most cases, the geometrical parameters of the formed halogen bonds fit into the optimal boundaries (Fig. 4, Table 3). The basic nitrogen atom still maintains a hydrogen bond with D98.

To further analyze the observed SAR, extensive molecular dynamics simulations were carried out for the most active derivatives (**8**, **9**, **35**, **36**, **37**, **41**). The starting poses were picked only from a group representing the second mode of binding, because only there halogen atoms may find a partner for interaction. For every investigated analog, the halogen atom quickly forms and maintains a directed interaction (numerical analysis of the geometrical parameters of halogen bonds is presented in Supplementary Information). For chlorine and bromine derivatives (**8**, **35**, **36**, **41**), the
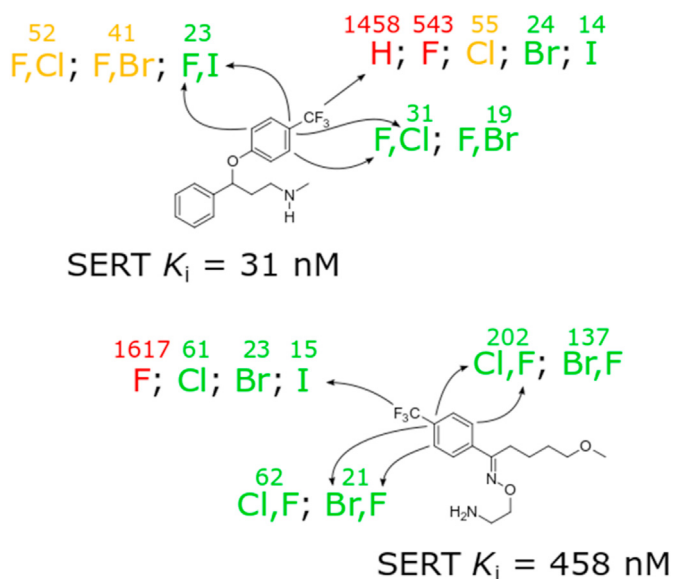
Fig. 2. Structure-activity relationship for the synthesized fluoxetine and fluvoxamine analogs. Binding affinity (K_i [nM]) is given above substituent symbols. Color codes represent general binding affinity change relative to trifluoromethyl reference compounds: red − large decrease, orange − moderate decrease, and green − no change or increase.
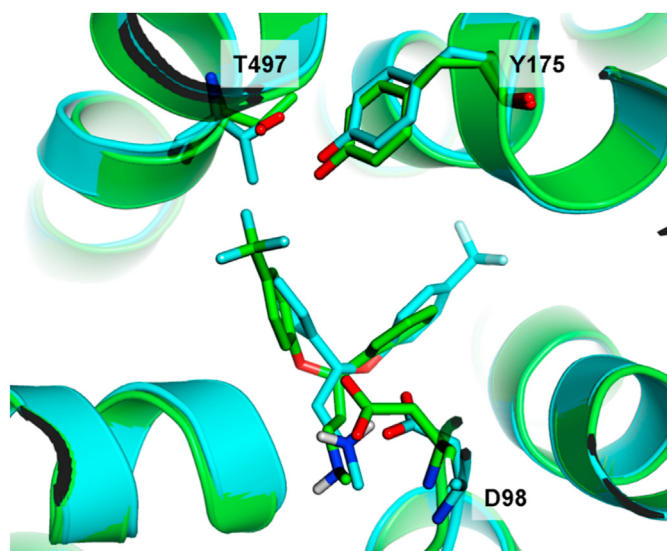
Fig. 3. Two ligand poses were obtained through IFD (compound **3** - fluoxetine as an example). A cyan structure marks a pose found in the SERT crystal structures. In this position, the trifluoromethyl group is located between helixes TM3 and TM8 and is surrounded by residues I172, A173, Y176, and L443. A green structure marks a pose that was a result of induced fit docking. Here, the trifluoromethyl group faces towards helix TM10.

interaction is formed with the backbone oxygen of G493 or T497. In the case of iodine derivative **37,** the halogen bond is also formed with the backbone oxygen of G493. In turn, the iodine derivative of fluoxetine **9** forms a halogen bond with the backbone oxygen of T497 and guanidine nitrogen of R104. To further investigate the correlation between the type of halogen atom and the strength of ligand-receptor interactions, the magnitude of the σ-hole was calculated (Table 2). The highest value is represented by compound **12** (45.7 kcal/mol), and the lowest value is represented by compound **6** (23.5 kcal/mol). Four analogs **9**, **12**, **37,** and **39** exhibit high

values (41.8, 45.7, 45.3, and 42.8, respectively), five analogs **11**, **14**, **36**, **38,** and **41** moderate values (37.3, 36.7, 37.10, 39.5, and 37.6, respectively) and another five analogs **8**, **10**, **13**, **35** and **40** low values (33.3, 33.4, 32.3, 33.5 and 33.4, respectively) of the σ-hole magnitude (a table with all of the data is shown in Supplementary Information).

3.3. Using XSAR sets to evaluate the role of halogens in Ligand−Protein complexes

Most of the identified halogen bonds are formed either with the T497 or E493 of SERT. The QPLD/GBSA (quantum-polarized ligand docking/generalized Born and surface area solvation) docking procedure and XSAR data were used to probe the SERT binding site to determine the amino acids most frequently targeted by halogen bonding. This particular methodology was previously used for a case study of the 5-HT$_7$ and D$_4$R receptors [22,23]. It is based on docking of a library of ligands to receptor proteins (either homology models or crystal structures) and subsequent analysis of ligand-receptor complexes with QPLD and GBSA. The obtained XSAR library for SERT was clustered into 79 sets and used to create an XSAR matrix showing positive changes in SERT activity upon exchange of hydrogen to halogen (simplified, representative data shown in Table 4, full matrix shown in Supplementary Information). We found one primary (E493) and three secondary (T497, S438, and S439) halogen bonding hot spots (a representative binding mode of two selected sets of compounds is presented in Fig. 5). The average increase in activity caused by the halogen bonds is equal to 95.52, whereas the median activity increase is equal to 8.3. A remarkable 1885-fold change in activity was recorded for set177, where two vicinal chlorine atoms formed two halogen bonds with E493 and T497. Similarly, two chlorine atoms in set124 yielded a 1760-fold increase in activity.

3.4. Synthesis of 3,4-dichloro analogs of fluoxetine and fluvoxamine

The outstanding activity reported for compounds with two vicinal chlorine atoms prompted us to synthetize 3,4-dichloro analogs of fluoxetine and fluvoxamine. The synthesis of both compounds was performed according to Scheme 1 (see Supplementary Information). To our great surprise, both derivatives were found to be more active than the best binding 4-iodo analog (Table 5). The Xeffect of compound **42** is equal to 291 (compared to compound **2**). Compound **46** is 51-fold more active than the parent fluvoxamine (compound **33**). To visualize the halogen bond interactions responsible for the increase in activity, induced fit docking was performed (Fig. 6).

3.5. Quantum mechanics calculations

The intriguing binding affinity changes, observed in the synthesized series of compounds, prompted us to perform a thorough analysis of the nature of interactions formed by halogen atoms with the transporter residues. Because of the extensiveness of the calculations, only a series of mono-substituted fluoxetine analogs (compounds **4**, **6**, **8**, **9**), supplemented by the dichloro analog (compound **42**), were selected for this task. First, the refined poses obtained from the IFD were again refined using quantum mechanics methods. The obtained poses were subjected to the extended transition state-natural orbitals for chemical valence (ETS-NOCV) and Bader's quantum theory of atoms in molecules (QTAIM) analyses [24−26]. As a result, decomposition of halogen interaction energy was obtained (Table S5, Supplementary Information). The QTAIM analysis allowed us to identify that, in addition to halogen bonds, hydrogen bonds are also a large contributor to
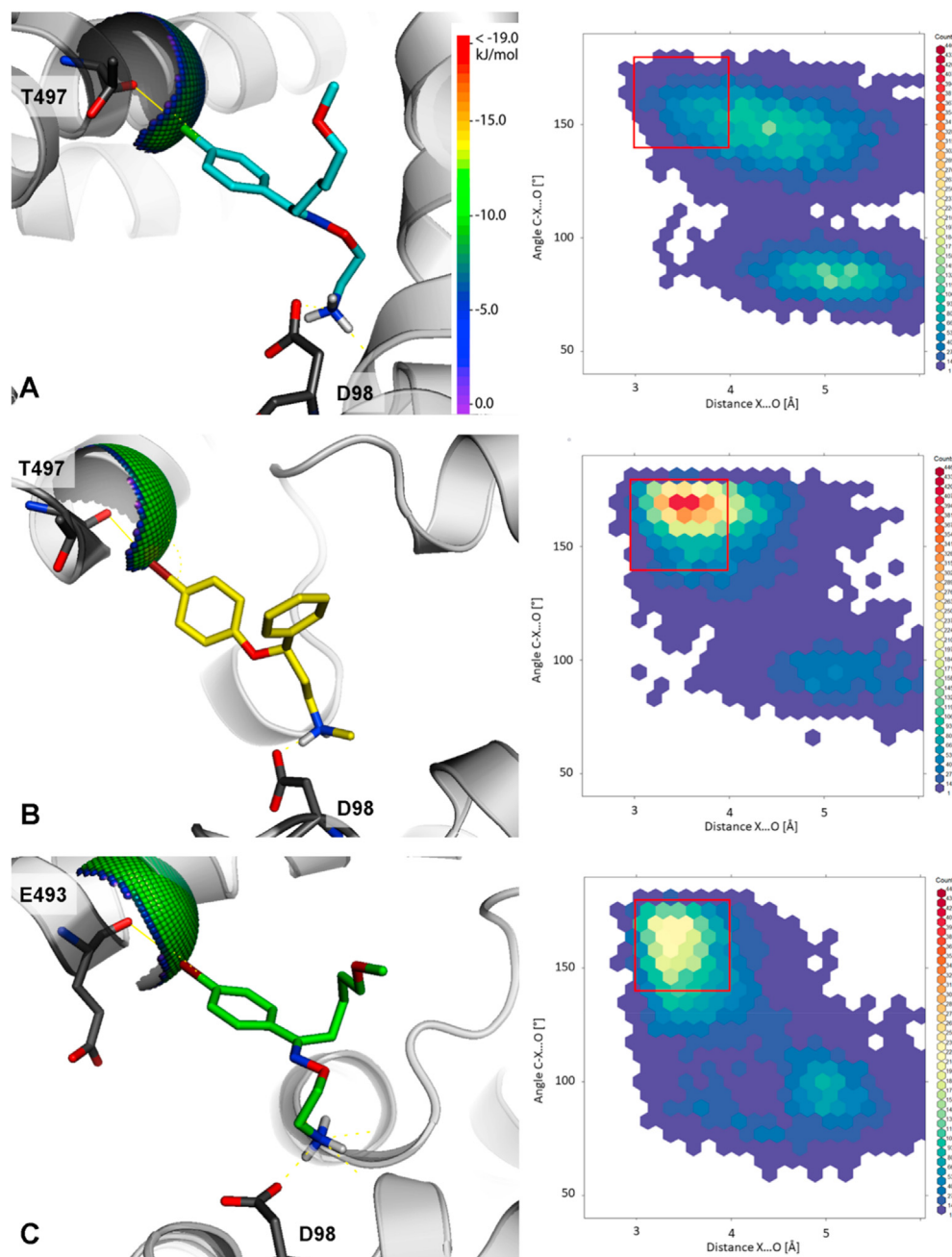
Fig. 4. Halogen bonds that were identified through the induced fit docking experiment. Next, to each figure, a 2D heat map representation of a halogen interaction is given, and the red rectangle marks the best geometric parameters of the interaction, i.e., 140° < angle <180° and 3 Å< distance <4 Å. (A) The chlorine atom of **35** forms a halogen bond with a backbone oxygen of T497, the distance X … O = 3.12 Å, the angle C−Cl···O = 172.3°; (B) the bromine atom of **8** forms a halogen bond with a backbone oxygen of G493, the distance X … O = 3.09 Å, the angle C−Br···O = 172.3°; (C) the bromine atom of **36** forms a halogen bond with a backbone oxygen of G493, the distance X … O = 3.15 Å, the angle C−Br···O = 172.3°. The chlorine(bromine)−oxygen theoretical interaction sphere illustrates the projected qualities of the formed L−R halogen bonds.

Table 2
Calculated values of the magnitude of σ-hole [kcal/mol] (σ-hole mgnd).

Fluoxetine analogs								
Cmpd	**6**	**10**	**13**	**8**	**11**	**14**	**9**	**12**
Halogen substitution pattern	4Cl	4Cl2F	4Cl3F	4Br	4Br2F	4Br3F	4I	4I2F
σ-hole mgnd [kcal/mol]	29.7	33.4	32.3	33.5	37.3	36.7	41.8	45.7

Fluvoxamine analogs							
Cmpd	**35**	**38**	**40**	**36**	**39**	**41**	**37**
Halogen substitution pattern	4Cl	4Cl2F	4Cl3F	4Br	4Br2F	4Br3F	4I
σ-hole mgnd [kcal/mol]	33.5	39.5	33.4	37.1	42.8	37.6	45.3

Table 3
Average geometric (distance and angle) parameters of halogen bonds formed between halogens of investigated structures and amino acids of the SERT, measured during 100 ns of performed molecular dynamics. The most optimal parameters of halogen bonds were described as distance <4.25 Å and angle >135° for iodine; distance <3.75 Å and angle >145° for bromine; distance <3.75 Å and angle >150° for chlorine [11].

Compound	X atom	Amino acid	Distance X … A [Å]	Angle C-X … A [°]
8	Br	T497	3.74 ± 0.41	161.78 ± 12.88
9	I	T497	4.14 ± 0.38	137.88 ± 9.62
		R104	3.76 ± 0.37	87.34 ± 9.19
35	Cl	T497	4.43 ± 0.64	148.08 ± 12.03
36	Br	T497	3.97 ± 0.75	136.34 ± 30.24
37	I	E493	4.95 ± 0.97	121.70 ± 11.33
41	Br	E493	4.17 ± 0.87	134.63 ± 28.08

the interaction with the transporter (a representative data for compound **42**, shown in Fig. 7, full results in Supplementary

Information pages 20−24). For the mono-chlorine derivative **6**, halogen bonds share 40% of the total interaction energy. This contribution increases slightly with the size of the halogen atom, reaching 43% and 54% for the bromine **8** and iodine **9** analogs, respectively. In turn, for the most active vicinal di-Cl analog **42**, the hydrogen bonds are responsible for 61% of the total interaction energy Apart from the above, we also observed the presence of X-HBD (halogen − hydrogen bond donor interaction, expressed also as HBeXB − HB enhanced XB [27]), formed between halogen atoms and hydroxyl group of threonine T497 or tyrosine Y175. Such interactions have already been recognized as being highly favorable to the ligand-protein interactions, through the enhancement of halogen bonds energies [28,29]. In our study, for the most active compound **42**, this interaction has the highest overall contribution to the binding energy (−5.0 and −1.7 kcal/mol, formed with a side chain of T497, simultaneously). Meanwhile, in the case of an iodine analog **9**, XB and X-HBD interactions have equal contribution in the

Table 4
A representative simplified XSAR matrix (full matrix shown in Supplementary Information) generated for 79 sets showing positive changes in SERT activity upon exchange of hydrogen with halogens: chlorine, bromine or iodine. Values depicted under aa. represent scoring functions that rate the quality of interaction; a value equal to 1 correlates with the most favorable and 0.25 for the least favorable interaction. Orange color states for a halogen bond formed with a backbone carbonyl oxygen, green for a halogen bond formed with a heteroatom at side chain of an amino acid and blue for a hybrid halogen-hydrogen bond formed either with a backbone or side chain. The sum of all scoring values is equal to 104.5. At the bottom of the table, this value is used to rate the frequency of interactions with particular amino acids. Most frequently, halogen bonds are formed with E493 (primary halogen bonds). The average activity increase for hydrophobic interactions is 4.81, for the halogen bond interaction is 95.52, whereas for halogen-hydrogen bonds, it is 141.45.

set_ID	\multicolumn{4}{c}{n-fold change in activity upon introduction of halogen (Xeffect)}	\multicolumn{8}{c}{Amino acid that is an acceptor of the halogen bond}	comments
	H	Cl	Br	I	E493	T497	S438	S439	S336	T175	T176	
set484	1	158.8	0	0	0.75			0.5		0.75		two XBa
set1534	1	132.5	0	0	1		0.75					CBb
set1683	1	31.3	0	0	0.75			0.5				CBb
set117	1	36.7	55	0	0.75							
	1	165	0	0	0.75	0.5						
	1	1885.7	0	0	1	0.75	0.5					two XBa
	1	2.3	0	0								HBIc
	1	2.8	0	0								HBIc
set124	1	106.9	381.3	0			0.75					
	1	1760	0	0	1	0.75						two XBa
set211	1	41,8	41,6	0	0.5					1		
	1	131,5	0	0	1	0.5						
	1	6,4	0	0								HBIc
set141	1	1.5	2.5	0				0.75				
	1	5	0	0			0.75					
set204	1	258.4	256.4	0	1					1		
	1	21.7	0	0	1	0.5						
set561	1	33.2	0	0						1		HBIc
	1	945	0	0	0.75	0.5				0.75		two XBa
	1	700	0	0	0.75							
set937	1	666.7	0	0	1	0.5	1					two XBa
set1047	1	91.8	0	0	1							
…	
sum					46	7.75	8.25	11.25	14	1.25	16	0	
total scored	104.5	0.44	0.07	0.08	0.11	0.13	0.01	0.15	0.00			

aXB –halogen bond; bCB – competitive binding, the halogen bond is formed alternatively with different partners; c HBI – hydrophobic interaction, d values given for complete data (Supplementary Information, page 11).

R	IC$_{50}$ [nM]
H	5655
2-Cl	881
3-Cl	135
4-Cl	43

R	IC$_{50}$ [nM]
H	>10 000
3,4-diCl	15
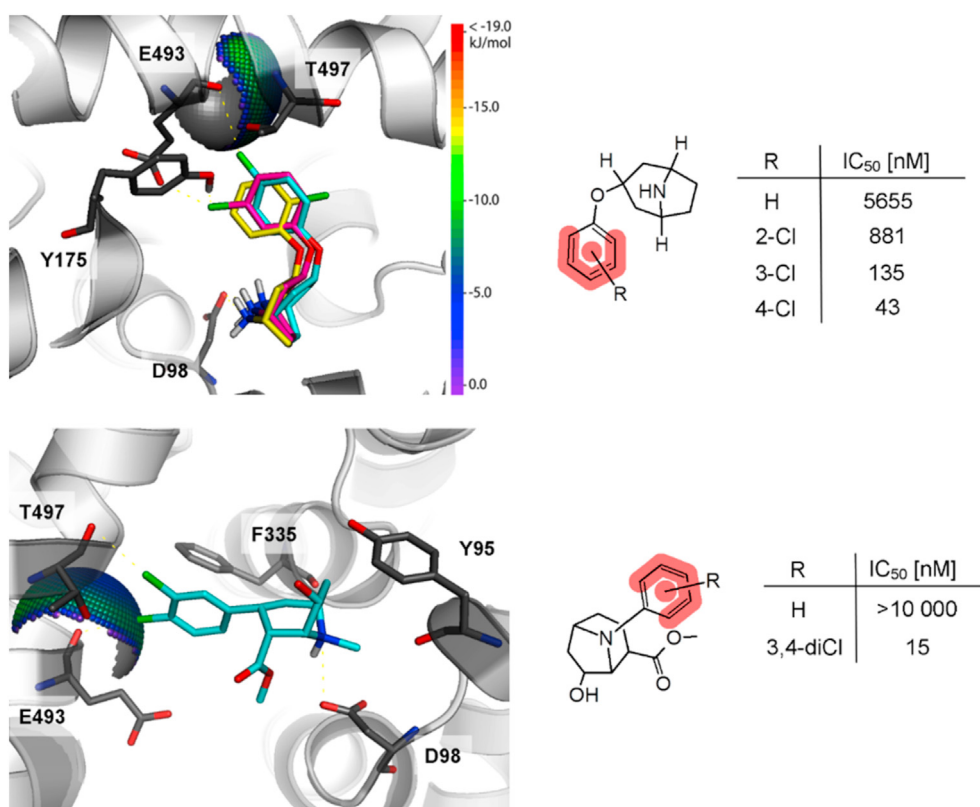
Fig. 5. The binding modes of the two selected major increases in the biological activity of SERT ligands upon the introduction of a halogen atom. In the upper example, walking the chlorine around the phenyl ring (XSAR set211) increased the IC$_{50}$ value 131-fold (compared with the derivative with no substituents) through the formation of a halogen bond with backbone oxygen of E493. The lower part of the figure represents a compound possessing two chlorine atoms in the meta and para positions (XSAR set937) that form two halogen bonds, with E493 and T497. This halogen arrangement causes a 666-fold increase in activity at SERT.

Table 5
Binding affinity values for synthesized 3,4-dichloro analogs of fluoxetine and fluvoxamine.

Cmpd	Structure	SERT K_i [nM]
42		**5**
46		**9**
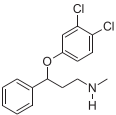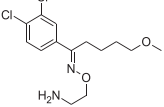
Binding affinity, K_i, expressed as the average of at least two independent experiments; the maximum S.D. did not exceed 10% (see Supplementary Information, page 20, Table 4).

L-P complex stabilization (−1.4, −1.3 kcal/mol, respectively). The HBs with methyl group also seem to significantly impact the binding because their energy ranges from −0.31 to −3.54 kcal/mol (the highest value is observed for dichloro analog). In turn, ETS-NOCV analysis showed that dispersion energy takes a high share of the total stabilization energy (Table S5, Supplementary Information), especially when HB is observed (X−HC HB takes approximately 30% of the total attractive energy for Br analog **8**). Compared to that, the halogen bonds have a very low dispersion energy component (~3%), while for X-HBD, this energy oscillates between XB and HB (from 9% to 26%).

4. Discussion

The analysis of the data collected for the synthesized compounds shows a strong correlation between the type of introduced halogen atom and SERT binding affinity. Chlorine analogs are among the least active compounds, while iodine analogs are the most active ones (Fig. 2). The influence of an additional fluorine atom placed in the 2- or 3- position relative to the halogen atom is more complex. From these two positions, only the ortho mutual orientation is favorable. In the case of fluoxetine chlorine analog **6** (SERT K_i = 55 nM), additional fluorine in the meta position (compound **10**, SERT K_i = 52 nM) has a negligible influence on the binding affinity. However, switching the fluorine to the 2-position (compound **13**) increases the binding affinity 1.77-fold. A different relationship was observed in the series of fluvoxamine analogs. Here, all chlorine derivatives are more active than the parent compound, with the 3-fluorine analog **38** the least active out of three (SERT K_i = 202 nM). The other two compounds, mono-chlorine and ortho-fluorine analogs, exhibit identical binding affinity and are 7.4-fold more active (SERT K_i = 61 nM and 62 nM, respectively) than fluvoxamine (SERT K_i = 458 nM). Interestingly, the introduction of bromine brings both fluoxetine and fluvoxamine analogs to an identical level of activity (average K_i = 21.75 ± 1.92 nM). Similar to the chlorine analogs, the only difference can be observed among the meta-fluorine derivatives (**11** and **39**); in both sets of derivatives, they are the least active (fluoxetine analog **11** SERT K_i = 41 nM, fluvoxamine analog **39** SERT K_i = 137 nM). Additionally, the incorporation of iodine into the structure of these SSRIs produces identically active compounds (fluoxetine analog **9** SERT K_i = 14 nM, fluvoxamine analog **37** SERT
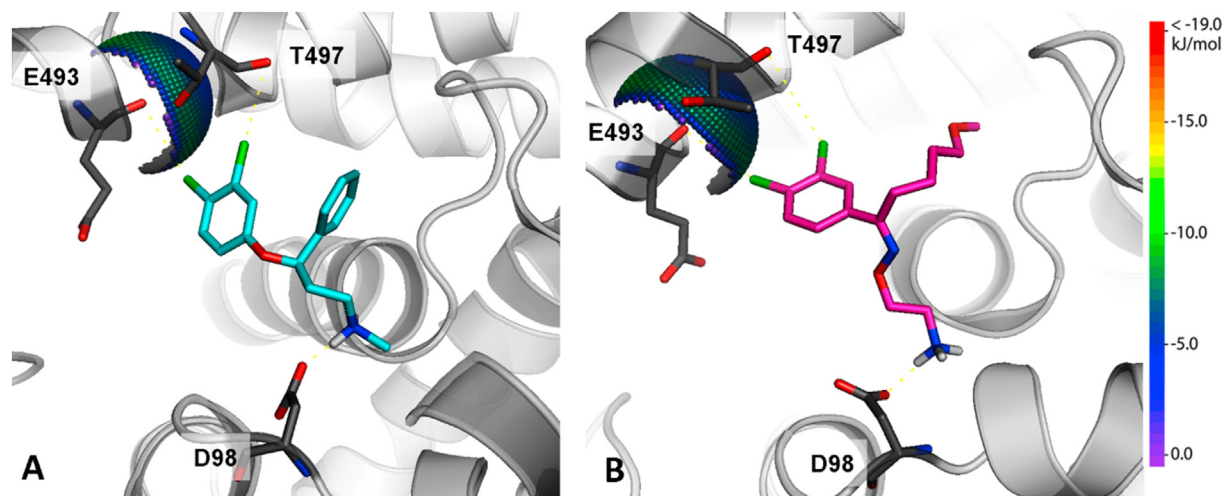
Fig. 6. Ligand-receptor complexes obtained through an induced fit docking of two 3,4-dichloro analogs of fluoxetine (compounds **42**, left, cyan) and fluvoxamine (compound **46**, right, magenta). Both compounds interact with the receptor via double halogen bonds formed with backbone carbonyl oxygen atoms of glutamic acid E492 and threonine T497. Such interactions caused a substantial increase in binding affinity for the receptor. Compound **42** is 291-fold more active than the analog without any substituent (compound **3**), and it is the most active SERT ligand presented in this manuscript. Compound **46** is 51-fold more active than the parent CF₃-containing fluvoxamine (compound **33**), and it is the second most active compound in this manuscript.
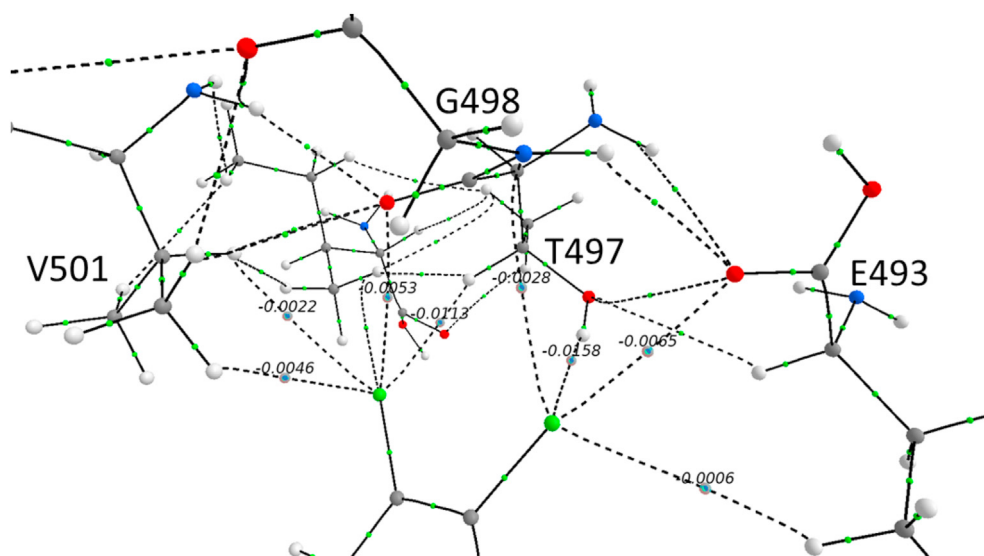
Fig. 7. The identified interactions of the halogen atom with the transporter residues, calculated using the QTAIM analysis, exemplified by compound **42**. On the image, individual interactions between halogen and the transporter are depicted as dotted lines. Next to each line, a value representing the share of total interaction energy is presented. The hydrogen bonds account for 70% of total interaction energy, while the halogen bonds for 30%.

K_i = 15 nM). As with the previous examples, 3-fluorine in **12** slightly lowers (1.64-fold) the binding affinity compared to a mono-iodine analog **9**. The average geometrical parameters (Table 3) of the halogen bonds during molecular dynamics do not fit precisely into the boundaries of the optimum values. Instead, they oscillate on the borders of the estimated optimum range. These results do not mean that above this range this interaction is not present, rather its strength is lowered by the unfavorable geometries. The increased affinity of compounds with heavier halogens leads to the conclusion that the size of the σ-hole may be the factor responsible for the affinity changes. Indeed, calculated values of the magnitude of the σ-hole correlate well with the activity of mono-substituted derivatives. The introduction of a fluorine atom increases this value in most cases, which surprisingly does not translate to a higher binding affinity. For example, compound **39** with a σ-hole

magnitude equal to 42.8 kcal/mol, similar to the most active iodine derivatives, is 9.8-fold less active. The additional fluorine atom, despite increasing the magnitude of the σ-hole, must be involved in other interactions that impair the binding of a ligand to the receptor.

The performed QTAIM analysis showed that the most important interaction in the analyzed complexes is represented by the X-HBD interactions. Those interactions seems to be a hybrid of XB and HB which results in a stronger interaction than the individual ones. The most optimum geometrical orientation for X-HBD is found for the C-X … HBD angle equal to 90° [30]. A query of the PDB repository allowed us to identify examples that incorporate non-halogenated compounds (2Q6H, 2QU3, 2WHO), for which it has been experimentally shown that adding a Cl or Br atom to the ligand significantly improves the binding affinity (even 200-fold), by creating X-

HBD [28]. The QTAIM analysis showed that X-HBD interaction between Cl and hydroxyl group of T497 has the highest values of energy stabilization (-1.7, -5.0 kcal/mol, for **7** and **42**, respectively). This feature of the chlorine atom translate to the formation of a very strong X-HBD interactions, which were found to be responsible for the high binding affinity of 3,4-diCl analogs. In spite of the complex nature of X-HBD, pure HB and XB can also be observed in the analyzed L-P complexes. In that case, importance of XBs increase along with the halogen atom size, with simultaneous decreased contribution of HBs (only 6% for iodine analog **9**) (Table S5, Supplementary Information). For all of the discussed interactions the dispersion energy is a vital component, however its share is strongly related to the type of the interaction. It is worth to note at this point, that the obtained QM refined poses constitute of the most optimum ligand-receptor mutual orientation and are probably poorly populated in the real time ligand-receptor interactions. Despite that, this type of analysis still allows to deeply investigate the binding of a ligand to the receptor.

All of the above observations lead to the hypothesis that starting from bromine, the halogen-receptor interaction becomes a dominant factor influencing the activity of these two SSRIs. Chlorine analogs **6** and **35** also possess similar binding affinity (SERT $K_i = 55$ nM and $K_i = 61$ nM, respectively), but the effect is less profound. The trifluoromethyl group interactions with the protein are weak and indirect; thus, structural differences of fluoxetine and fluvoxamine produce a very distinct binding affinity (SERT $K_i = 31$ nM and $K_i = 458$ nM, respectively). The ability of heavier halogen atoms to form a direct interaction causes different chemical scaffolds of these compounds to lose their decisive impact on the activity. The molecular modeling experiments showed two distinct binding modes (Fig. 3). Here, the increase in activity brought by the introduction of a halogen atom can be explained on the ground of the formed halogen atom interactions, which are possible only in the alternative binding mode (Fig. 3). Most frequently, these interactions were formed with either T497 or E493. To date, only one halogen bond in the SERT complex has been reported. In 2019, Abramyan et al. showed a complex of bromo paroxetine with SERT, where the bromine atom pointed in the direction of the E493 and T497 backbone oxygens. However, no further analysis was performed [31]. Therefore, we performed an XSAR analysis, which showed explicitly that E493 was the most frequently targeted amino acid in terms of halogen bonding with SERT. Moreover, the proximity of T497 and E493 allowed for the formation of two strong interactions with two vicinal halogen atoms. Such an optimal arrangement in some cases resulted in a spectacular thousand-fold increase in biological activity (Table 4). This finding supported our hypothesis for the alternative binding mode of SERT ligands bearing heavier halogen atoms. Finally, two synthesized 3,4-dichloro analogs of fluoxetine and fluvoxamine confirmed the theoretical assumption and showed a marked increase in activity. Fluoxetine analog **42** was 3-fold more active and fluvoxamine analog **46** was 1.7-fold more active than the best-binding 4-iodo analogs.

5. Conclusions

In the present study, a series of fluoxetine and fluvoxamine analogs with varying patterns of halogen substitution were synthesized, and their biological activities were measured. Among the synthesized initial series of compounds, a classical order of increasing activity from chlorine to iodine was observed. Introduced additional fluorine atoms did not have a substantial influence on the affinity for the receptor. Subsequent thorough *in silico* analysis of the binding modes indicated the possibility of the formation favorable X-HBD interactions with the residues E493 and

T497. This type of interaction was found to be a hybrid of XB and HB interactions, with the latter accounting for a higher share of the interaction energy. Subsequently, the use of an XSAR analysis allowed to translate this to a general rule governing the binding of SERT ligands. Especially interesting was the observation that SERT ligands with heavier halogens bind via a markedly different, "switched" binding mode than the parent trifluoromethyl analogs. To the best of our knowledge, no paper to date has exclusively reported two distinct binding modes for SERT ligands. Finally, the given hypothesis of halogen bond type interactions with the receptor was confirmed by the experimental measurement of the affinity constant for 3,4-dichloro analogs of fluoxetine and fluvoxamine, which were the most active among all of the synthesized compounds. The presented manuscript states as an example of the successful use of molecular modeling for the analysis and optimization of compound activity. The utilized tool, XSAR analysis, previously used for the 5-HT$_7$R [22] and D$_4$R ligands [22,23], proved to be universal and applicable for a broader type of biological target. We anticipate that such a methodology could be successfully utilized for the structure optimization of any halogen-containing biologically active compound.

Declaration of competing interest

The authors declare that they have no known competing financial interests or personal relationships that could have appeared to influence the work reported in this paper.

Acknowledgments

Appendix A. Supplementary data

Supplementary data to this article can be found online at https://doi.org/10.1016/j.ejmech.2021.113533.

Methodology

Structure−activity relationship datasets for halogenated analogs

An algorithm to find all pairs containing halogenated and corresponding unsubstituted structures (called the XSAR library) was developed and used for the 5-HT$_7$ and D$_4$ targets in our previous studies [22]. To describe the influence of halogenation on the biological activity of the unsubstituted (parent) molecule, the Xeffect parameter was calculated as an activity (extracted from the ChEMBL database during the generation of the XSAR library) ratio of the parent compound to its halogenated derivative (an Xeffect between 0 and 1 denotes a decrease in the activity upon halogenation, and an Xeffect greater than 1 means the fold of activity increased after halogen substitution).

Identification of halogen bonding hot spots for SERT

Privileged amino acids (i.e., hot spots) for halogen bonding were identified using a procedure including the following steps: clustering the halogenated analogs representing each XSAR set, using the centroids of the clusters to tune the SERT binding site by an induced-fit docking procedure, QPLD docking of the XSAR library to

SERT conformations, and determination of the number of halogen bonding interactions with the side chains and carbonyl oxygen atoms of amino acids in the docking poses.

Induced fit docking

The structure of the ts3 human serotonin transporter in complex with paroxetine (PDB code 5I6X) was retrieved from the Protein Data Bank [20]. Wild-type human SERT is unstable in detergent solutions during crystallization, so all crystal structures in PDB repositories consist of thermostable mutants. The ts3 mutant of the human serotonin transporter contains three thermostabilizing mutations, namely, I291A, T439S, and Y110A. To obtain reliable results from docking and molecular dynamics, the native amino acid sequence was restored using Schrodinger software.

The three-dimensional structures of ligands were prepared using LigPrep v3.6 [32]' and the appropriate ionization states at pH = 7.0 ± 0.5 were assigned using Epik v3.4 [33]. The Protein Preparation Wizard was used to assign the bond orders and appropriate amino acid ionization states and to check for steric clashes. All ligands were docked using the induced fit docking (IFD) [34,35] protocol with XP with an OPLS3e force field. The L−R complexes selected in the IFD procedure were next optimized using the QM/MM approach with QSite [34,36]. The QM area containing ligand and the conserved amino acid side chain was described by a combination of DFT hybrid functional B3LYP and LACVP* basis set, while the rest of the system was optimized using the OPLS2005 force field.

Molecular dynamics

Molecular dynamics (MD) simulations were performed using Schrödinger Desmond software [37]. Each ligand−receptor complex, optimized in the QM/MM procedure, was immersed into a POPC (300 K) membrane bilayer, whose position was calculated using the System Builder interface. The system was solvated by water molecules described by the TIP4P potential, and the OPLS3e [38] force field parameters were used for all atoms. NaCl (0.15 M) was added to mimic the ionic strength inside the cell. Molecular simulations for 100 ns (recording frames 10 ps and step of 2 fs) using the NPAT ensemble class (constant normal pressure, temperature, and lateral surface area of membranes) and OPLS3e [39] force field were calculated for each system. Based on the obtained trajectories, the mean geometrical distances between amino acids and ligands were calculated using Simulation Event Analysis tools in Maestro Schrödinger Suit.

Magnitude of σ-hole

MultiWFN [40,41] software was used to calculate the size of the sigma hole for selected fluvoxamine and fluoxetine derivatives. First, DFT [42] structure optimization was performed with the Gaussian 16 package at the M06-2X [43]/def2-qZVP [44] level of theory with the polarizable continuum model (PCM) [45,46] (solvent = water). The obtained wave functions were used to calculate the values of maximum electrostatic potential over the isodensity surface with MultiWFN as an approach to quantifying the σ-holes.

QTAIM analysis

For chosen complexes, the ligands and all residues in the range of 4 Å from halogen atom were extracted and the QTAIM [47] calculations (Quantum Theory of Atoms in Molecule) were performed. The electron density topological analysis was carried out with the AIMAll [48] program, based on electron density calculated with

Gaussian G16 at the M06-2X/def2-tzvp [43,49] level of theory. The energy of non-covalent bonds detected in crystal structures was calculated with the Espinosa equation [50]:

$$E_{int} = \frac{1}{2}v(r)$$

where E_{int} is the energy of interatomic interaction (a.u.) and $v(r)$ is kinetic energy in the bond critical point (BCP).

ETS-NOCV

To fully characterize obtained interactions we used an approach for energy decomposition analysis. The bonding analysis was performed using the ETS-NOCV approach the extended transition state (ETS) method [51] with the natural orbitals for the chemical valence (NOCV) scheme [52−54]. In this approach the total energy of bonding between the interacting molecules (ΔE_{int}) is divided into following contributions:

$$\Delta E_{int} = \Delta E_{dist} + \Delta E_{el} + \Delta E_{Pauli} + \Delta E_{orb}$$

where ΔE_{dist} is energy required to promote the separated fragments from their equilibrium geometry to the structure they will take up in the complex, ΔE_{el} is corresponding to the electrostatic interaction between the two fragments in the supermolecule geometry, ΔE_{Pauli} is the repulsive interaction between occupied orbitals of the two fragments, and the orbital interaction term and ΔE_{orb} is representation of the stabilizing component due to the final orbital relaxation. All calculations were performed using the using the Amsterdam Density Functional (ADF) program [55−58], implementing the ETS-NOCV scheme. The BLYP-D3 [59] [16] functional and a standard double-ζ STO basis containing one set of polarization functions was adopted for all the electrons (TZP), were used in calculations.

Plotting interaction spheres for halogen bonding

To visualize (plotting interaction spheres) the possible contribution of halogen bonding to L−R complexes, the halogen bonding Web server was used (accessed June 20, 2020, http://www.halogenbonding.com/) [60].

Radioligand binding replacement experiment

Cell culture and preparation of cell membranes for radioligand binding assays

The HEK293 human serotonin transporter cell line (PerkinElmer) was maintained at 37 °C in a humidified atmosphere with 5% CO$_2$ and grown in Dulbecco's Modifier Eagle Medium containing 10% dialyzed fetal bovine serum and 500 μg/mL G418 sulfate. For membrane preparation, cells were subcultured in 150 cm^2 flasks, grown to 90% confluence, washed twice with phosphate buffered saline (PBS) prewarmed to 37 °C and pelleted by centrifugation (200×g) in PBS containing 0.1 mM EDTA and 1 mM dithiothreitol. Prior to membrane preparation, pellets were stored at −80 °C.

Radioligand binding assays

Cell pellets were thawed and homogenized in 10 vol of assay buffer using an Ultra Turrax tissue homogenizer and centrifuged twice at 35,000×g for 20 min at 4 °C. The composition of the assay buffer was as follows: 50 mM Tris-HCl pH 7.4, 120 mM NaCl, and 5 mM KCl. The assay was incubated in a total volume of 200 μl in 96-well microtiter plates for 0.5 h at 27 °C. The process of equilibration was terminated by rapid filtration through GF/C Unifilter plates (PerkinElmer) with a FilterMate Unifilter 96-Harvester

(PerkinElmer). The radioactivity bound to the filters was quantified on a Microbeta TopCount instrument (PerkinElmer). For competitive inhibition studies, the assay samples contained 3 nM [^{3}H]-citalopram (74.5 Ci/mmol). Non-specific binding was determined with 10 μM imipramine. Each compound was tested in triplicate at 7 concentrations (10^{-10}-10^{-4} M). The inhibition constants (K_i) were calculated from the Cheng-Prusoff equation [61]. For all binding assays, the results were expressed as the means of at least two separate experiments.

Synthesis

*A general procedure for the synthesis of compounds **2**−**14***

Tert-butyl *N*-(3-hydroxy-3-phenylpropyl)-*N*-methylcarbamate (0.0026 mol), appropriate phenol (1 eq.), Ph$_3$P (1.2 eq.) were added to a round bottom flask and dissolved in anhydrous THF (50 mL, distilled over LiAlH$_4$) and cooled on ice. Next, DIAD (1.2 eq.) was added dropwise. The reaction mixture was allowed to warm to room temperature and stirred overnight. The solvent was evaporated, and conc. H$_3$PO$_4$ (5 mL) was added; an evolution of gases was observed. The mixture was stirred for 3 h at room temperature, after which water was added (100 mL), and the mixture was extracted with EtOAc (3 × 50 mL). The aqueous layer was basified with 15% NaOH and extracted with EtOAc (3 × 50 mL). Combined organic extracts were washed with brine and dried over anhydrous MgSO$_4$. The product was purified using column chromatography in silica gel with EtOAc:MeOH (9:1).

*A general procedure for the synthesis of compounds **15**−**24***

Magnesium turnings (1.1 eq., 0.47 g) were grated in a mortar and placed in a round bottom flask under an Ar atmosphere. Anhydrous Et$_2$O (30 mL, distilled over LiAlH$_4$) was added with subsequent addition of ethylene bromide (0.1 eq., 0.155 mL). After 15 min at room temperature, 1-bromo-4-methoxybutane (3 g, 0.018 mol) was added portionwise. After all of the bromide reacted with the magnesium, the reaction mixture was cooled on ice, and a solution of appropriate benzonitrile (0.6 eq., 0.0107 mol) in anhydrous Et$_2$O (50 mL) was added portionwise. The reaction mixture was refluxed for 8 h. The reaction was quenched with ice-water and acidified with 6 N HCl. The organic layer was separated, and the aqueous phase was extracted with EtOAc (3 × 50 mL). The combined organic layers were washed with brine (50 mL), dried over MgSO$_4$, and evaporated. The crude product was purified by column chromatography on silica gel hexane:EtOAc (6:1) to give the title compound as an oil or solid.

*A general procedure for the synthesis of compounds **24**−**32***

To a solution of ketone (1 eq.) in EtOH (5 mL) hydroxylamine hydrochloride (2 eq.) and NaOAc (2 eq.) were added. After stirring at room temperature for 3 h, the reaction mixture was quenched with water (10 mL) and extracted with DCM (3 × 30 mL). The combined organic phases were dried over MgSO$_4$ and evaporated to dryness. The residue was purified by column chromatography on silica gel with hexane:EtOAc (5:1) to give the title compound.

*A general procedure for the synthesis of compounds **33**−**41***

An appropriate oxyme (1 mmol), 2-chloroethanamine hydrochloride (0.7 mmol), and KOH (1.5 mmol) were added to dry DMF (6 mL) at 10 °C. The reaction mixture was stirred overnight at room temperature. Next, the reaction mixture was concentrated to remove DMF, and then water was added (50 mL). The mixture was extracted with EtOAc (3 × 30 mL). The combined organic phases were washed with brine (20 mL), dried over MgSO$_4$, and evaporated to produce the target compound.

References

[1] K.P. Lesch, B.L. Wolozin, D.L. Murphy, P. Riederer, Isolation of a CDNA encoding the human brain serotonin transporter, J. Neurochem. 60 (1993) 2319−2322.

[2] S. Montanez, L.C. Daws, G.G. Gould, A. Frazer, Serotonin (5-HT) transporter (SERT) function after graded destruction of serotonergic neurons, J. Neurochem. 87 (2003) 861−867.

[3] S.M. Stahl, C. Lee-Zimmetman, S. Cartwright, D.A. Morrissette, Serotonergic drugs for depression and beyond, Curr. Drug Targets 14 (2013) 578−585.

[4] A. Caspi, K. Sugden, T.E. Moffitt, A. Taylor, I.W. Craig, H. Harrington, Influence of life stress on depression: moderation by a polymorphism in the 5-HTT gene, Science 301 (2003) 386−389 (80-.).

[5] T.C. Eley, K. Sugden, A. Corsico, A.M. Gregory, P. Sham, P. McGuffin, Gene-enviroment interaction analysis of serotonin system with adolescent depression, Mol. Psychiatr. 9 (2004) 908−915.

[6] G.R. Desiraju, P.S. Ho, L. Kloo, A.C. Legon, R. Marquardt, P. Metrangolo, P. Politzer, G. Resnati, K. Rissanen, Definition of the halogen bond (IUPAC recommendations 2013), Pure Appl. Chem. 85 (8) (2013) 1711−1713.

[7] V. Andrea, H. P, The role of halogen bonding in inhibitor recognition and binding by protein kinases, Curr. Top. Med. Chem. 7 (14) (2007) 1336−1348.

[8] L.A. Hardegger, B. Kuhn, B. Spinnler, L. Anselm, R. Ecabert, M. Stihle, B. Gsell, R. Thoma, J. Diez, J. Benz, et al., Systematic investigation of halogen bonding in protein-ligand interactions, Angew. Chem. Int. Ed. 50 (1) (2011) 314−318.

[9] K.E. Riley, J.S. Murray, R. Jan, R.J. Solá, M.C. Concha, F.M. Ramos, P. Politzer, J. Fanfrlík, J. Řezáč, R.J. Solá, et al., Halogen bond tunability II: the varying roles of electrostatic and dispersion contributions to attraction in halogen bonds, J. Mol. Model. 19 (11) (2013) 4651−4659.

[10] J. Fanfrlik, M. Kolar, M. Kamlar, D. Hurny, F.X. Ruiz, A. Cousido-Siah, A. Mitschler, J. Rezac, E. Munusamy, M. Lepsik, et al., Modulation of aldose reductase inhibition by halogen bond tuning, ACS Chem. Biol. 8 (2013) 2484−2492.

[11] R. Wilcken, M.O. Zimmermann, A. Lange, A.C. Joerger, F.M. Boeckler, Principles and applications of halogen bonding in medicinal chemistry and chemical biology, J. Med. Chem. 56 (2013) 1363−1388.

[12] P. Auffinger, F.A. Hays, E. Westhof, P.S. Ho, Halogen bonds in biological molecules, Proc. Natl. Acad. Sci. U. S. A. 101 (48) (2004) 16789−16794.

[13] J. Andersen, I. Olsen, K.B. Hansen, O. Taboureau, F.S. Jørgensen, A. Marie, B. Bang-andersen, J. Egebjerg, K. Strømgaard, A.S. Kristensen, Mutational mapping and modeling of the binding site for (S) -citalopram in the human serotonin transporter, J. Biol. Chem. 285 (3) (2010) 2051−2063.

[14] D.T. Wong, F.P. Bymaster, E.A. Engleman, Prozac (fluoxetine, lilly 110140), the first selective serotonin uptake inhibitor and and antidepressant drug: twenty years since its first publication, Life Sci. 57 (5) (1995) 411−441.

[15] S. Chumpradit, M.P. Kung, C. Panyachotipun, V. Prapansiri, C. Foulon, B.P. Brooks, S.A. Szabo, S. Tejani-Butt, A. Frazer, H.F. Kung, Iodinated tomoxetine derivatives as selective ligands for serotonin and norepinephrine uptake sites, J. Med. Chem. 35 (23) (1992) 4492−4497.

[16] H.B.A. Welle, V. Claassen, Aminoethyl Oximes Having Anti-depressive Activity, Patent US4086361A, 1978.

[17] O.M. Okunola-Bakare, J. Cao, T. Kopajtic, J.L. Katz, C.J. Loland, L. Shi, A.H. Newman, Elucidation of structural elements for selectivity across monoamine transporters: novel 2-[(Diphenylmethyl)Sulfinyl]Acetamide (modafinil) analogues, J. Med. Chem. 57 (3) (2014) 1000−1013.

[18] R.D. Slack, A.M. Abramyan, H. Tang, S. Meena, B.A. Davis, A. Bonifazi, J.B. Giancola, J.R. Deschamps, S. Naing, H. Yano, et al., A novel bromine-containing paroxetine analogue provides mechanistic clues for binding ambiguity at the central primary binding site of the serotonin transporter, ACS Chem. Neurosci. 10 (9) (2019) 3946−3952.

[19] Z. Zhou, J. Zhen, N.K. Karpowich, C.J. Law, M.E.A. Reith, D. Wang, Antidepressant specificity of serotonin transporter suggested by three LeuT − SSRI structures, Nat. Struct. Mol. Biol. 16 (6) (2009) 652−658.

[20] J.A. Coleman, E.M. Green, E. Gouaux, X-ray structures and mechanism of the human serotonin transporter, Nature 532 (7599) (2016) 334−339.

[21] J.A. Coleman, E. Gouaux, Structural basis for recognition of diverse antidepressants by the human serotonin transporter, Nat. Struct. Mol. Biol. 25 (2) (2018) 170−175.

[22] R. Kurczab, V. Canale, G. Satała, P. Zajdel, A.J. Bojarski, Amino acid hot spots of halogen bonding: a combined theoretical and experimental case study of the 5-HT7 receptor, J. Med. Chem. 61 (19) (2018) 8717−8733.

[23] R. Kurczab, K. Kucwaj-Brysz, P. Śliwa, The significance of halogen bonding in ligand−receptor interactions: the lesson learned from molecular dynamic simulations of the D4 receptor, Molecules 25 (1) (2019) 91.

[24] R.F.W. Bader, Atoms in molecules, Acc. Chem. Res. 18 (1) (1985) 9−15.

[25] R.F.W. Bader, Atoms in Molecules. A Quantum Theory, Clarendon Press, Oxford, UK, 1990.

[26] K. Dyduch, M.P. Mitoraj, A. Michalak, ETS-NOCV description of σ-hole bonding, J. Mol. Model. 19 (7) (2013) 2747−2758.

[27] A.M.S. Riel, R.K. Rowe, E.N. Ho, A.-C.C. Carlsson, A.K. Rappé, O.B. Berryman, P.S. Ho, Hydrogen bond enhanced halogen bonds: a synergistic interaction in chemistry and biochemistry, Acc. Chem. Res. 52 (10) (2019) 2870−2880.

[28] F.-Y. Lin, A.D. MacKerell, Do halogen−hydrogen bond donor interactions dominate the favorable contribution of halogens to ligand−protein binding? J. Phys. Chem. B 121 (28) (2017) 6813−6821.

[29] A.-C.C. Carlsson, M.R. Scholfield, R.K. Rowe, M.C. Ford, A.T. Alexander,

R.A. Mehl, P.S. Ho, Increasing enzyme stability and activity through hydrogen bond-enhanced halogen bonds, Biochemistry 57 (28) (2018) 4135−4147.

[30] R.K. Rowe, P.S. Ho, Relationships between hydrogen bonds and halogen bonds in biological systems, Acta Crystallogr. B 73 (2) (2017) 255−264.

[31] A.M. Abramyan, R.D. Slack, S. Meena, B.A. Davis, A.H. Newman, S.K. Singh, L. Shi, Computation-guided analysis of paroxetine binding to HSERT reveals functionally important structural elements and dynamics, Neuropharmacology 161 (2019) 107411.

[32] Schrodinger LigPrep, Release 2017-3, Schrodinger, LLC, NewYork, NY, 2017.

[33] Schrodinger Epik, Release 2017-3, Schrodinger, LLC, New York,NY, 2017.

[34] Schrödinger QSite, Release 2017-3, Schrödinger, LLC, New York,NY, 2017.

[35] W. Sherman, T. Day, M.P. Jacobson, R.A. Friesner, R. Farid, Novel procedure for modeling ligand/receptor induced fit effects, J. Med. Chem. 49 (2) (2006) 534−553.

[36] R.B. Murphy, D.M. Philipp, R.A. Friesner, A mixed quantum mechanics/molecular mechanics (QM/MM) method for large-scale modeling of chemistry in protein environments, J. Comb. Chem. 21 (16) (2000) 1442−1457.

[37] K.J. Bowers, F.D. Sacerdoti, J.K. Salmon, Y. Shan, D.E. Shaw, E. Chow, H. Xu, R.O. Dror, M.P. Eastwood, B.A. Gregersen, et al., Molecular dynamics—scalable algorithms for molecular dynamics simulations on commodity clusters, in: In Proceedings of the 2006 ACM/IEEE Conference on Supercomputing − SC '06, ACM Press, New York, New York, USA, 2006, p. 84.

[38] E. Harder, W. Damm, J. Maple, C. Wu, M. Reboul, J.Y. Xiang, L. Wang, D. Lupyan, M.K. Dahlgren, J.L. Knight, et al., OPLS3: a force field providing broad coverage of drug-like small molecules and proteins, J. Chem. Theor. Comput. 12 (1) (2016) 281−296.

[39] K. Roos, C. Wu, W. Damm, M. Reboul, J.M. Stevenson, C. Lu, M.K. Dahlgren, S. Mondal, W. Chen, L. Wang, et al., OPLS3e: extending force field coverage for drug-like small molecules, J. Chem. Theor. Comput. 15 (3) (2019) 1863−1874.

[40] T. Lu, F. Chen, Quantitative analysis of molecular surface based on improved marching tetrahedra algorithm, J. Mol. Graph. Model. 38 (2012) 314−323.

[41] T. Lu, F. Chen, Multiwfn: a multifunctional wavefunction analyzer, J. Comput. Chem. 33 (5) (2012) 580−592.

[42] M.J. Frisch, G.W. Trucks, H.B. Schlegel, G.E. Scuseria, M.A. Robb, J.R. Cheeseman, G. Scalmani, V. Barone, G.A. Petersson, H. Nakatsuji, X. Li, M. Caricato, A.V. Marenich, J. Bloino, B.G. Janesko, R. Gomperts, B. Mennucci, D.J. Hratch, Gaussian 16, Revision A.03. Gaussian 16, Revis. A.03, 2016.

[43] Y. Zhao, D.G. Truhlar, The M06 suite of density functionals for main group thermochemistry, thermochemical kinetics, noncovalent interactions, excited states, and transition elements: two new functionals and systematic testing of four M06-class functionals and 12 other function, Theor. Chem. Acc. 120 (1−3) (2008) 215−241.

[44] F. Weigend, R. Ahlrichs, Balanced basis sets of split valence, triple zeta valence and quadruple zeta valence quality for H to Rn: design and assessment of accuracy, Phys. Chem. Chem. Phys. 7 (18) (2005) 3297.

[45] B. Mennucci, R. Cammi, J. Tomasi, Analytical free energy second derivatives with respect to nuclear coordinates: complete formulation for electrostatic continuum solvation models, J. Chem. Phys. 110 (14) (1999) 6858−6870.

[46] S. Miertuš, E. Scrocco, J. Tomasi, Electrostatic interaction of a solute with a continuum. A direct utilizaion of AB initio molecular potentials for the prevision of solvent effects, Chem. Phys. 55 (1) (1981) 117−129.

[47] W.A. Waters, Vistas of organic chemistry, Nature 173 (4413) (1954) 1012−1013.

[48] A. Todd, T.G.S. Keith, AIMAll. Overland Park KS: USA, 2019.

[49] M.K. Kesharwani, B. Brauer, J.M.L. Martin, Frequency and zero-point vibrational energy scale factors for double-hybrid density functionals (and other selected methods): can anharmonic force fields Be avoided? J. Phys. Chem. 119 (9) (2015) 1701−1714.

[50] E. Espinosa, E. Molins, C. Lecomte, Hydrogen bond strengths revealed by topological analyses of experimentally observed electron densities, Chem. Phys. Lett. 285 (3−4) (1998) 170−173.

[51] T. Ziegler, A. Rauk, On the calculation of bonding energies by the Hartree Fock slater method, Theor. Chim. Acta 46 (1) (1977) 1−10.

[52] A. Michalak, M. Mitoraj, T. Ziegler, Bond orbitals from chemical valence theory, J. Phys. Chem. 112 (9) (2008) 1933−1939.

[53] M. Mitoraj, A. Michalak, Applications of natural orbitals for chemical valence in a description of bonding in conjugated molecules, J. Mol. Model. 14 (8) (2008) 681−687.

[54] M. Mitoraj, A. Michalak, Natural orbitals for chemical valence as descriptors of chemical bonding in transition metal complexes, J. Mol. Model. 13 (2) (2007) 347−355.

[55] G. te Velde, F.M. Bickelhaupt, E.J. Baerends, C. Fonseca Guerra, S.J.A. van Gisbergen, J.G. Snijders, T. Ziegler, Chemistry with ADF, J. Comput. Chem. 22 (9) (2001) 931−967.

[56] E.J. Baerends, P. Ros, Self-consistent molecular Hartree—Fock—slater calculations II. The effect of exchange scaling in some small molecules, Chem. Phys. 2 (1) (1973) 52−59.

[57] E.J. Baerends, D.E. Ellis, P. Ros, Self-consistent molecular Hartree—Fock—slater calculations I. The computational procedure, Chem. Phys. 2 (1) (1973) 41−51.

[58] G. te Velde, E.J. Baerends, Numerical integration for polyatomic systems, J. Comput. Phys. 99 (1) (1992) 84−98.

[59] J.P. Finley, Using the local density approximation and the LYP, BLYP and B3LYP functionals within reference-state one-particle density-matrix theory, Mol. Phys. 102 (7) (2004) 627−639.

[60] R. Wilcken, M.O. Zimmermann, A. Lange, S. Zahn, F.M. Boeckler, Using halogen bonds to address the protein backbone: a systematic evaluation, J. Comput. Aided Mol. Des. 26 (8) (2012) 935−945.

[61] Y.-C. Cheng, W.H. Prusoff, Relationship between the inhibition constant (KI) and the concentration of inhibitor which causes 50 per cent inhibition (I50) of an enzymatic reaction, Biochem. Pharmacol. 22 (23) (1973) 3099−3108.